Interpretation of Molecular Dynamics on Different Time Scales in Unilamellar Vesicles Using Field−Cycling NMR Relaxometry

ARTICLE *in* THE JOURNAL OF PHYSICAL CHEMISTRY B · NOVEMBER 2009

Impact Factor: 3.3 · DOI: 10.1021/jp907084s · Source: PubMed

5 AUTHORS, INCLUDING:

Josefina Perlo
RWTH Aachen University
15 PUBLICATIONS **174** CITATIONS
SEE PROFILE

Ezequiel Farrher
Forschungszentrum Jülich
10 PUBLICATIONS **100** CITATIONS
SEE PROFILE

Dermot Brougham
Dublin City University
63 PUBLICATIONS **1,026** CITATIONS
SEE PROFILE

Interpretation of Molecular Dynamics on Different Time Scales in Unilamellar Vesicles Using Field-Cycling NMR Relaxometry

Carla J. Meledandri,[†] Josefina Perlo,[‡] Ezequiel Farrher,[‡] Dermot F. Brougham,*[,†] and Esteban Anoardo*[,‡]

National Institute for Cellular Biotechnology, School of Chemical Sciences, Dublin City University, Dublin 9, Ireland, and Larte - Famaf. Universidad Nacional de Córdoba and Instituto de Física Enrique Gaviola (CONICET), Córdoba, Argentina

Received: July 24, 2009; Revised Manuscript Received: October 14, 2009

Fast field-cycling (FFC) and rotating-frame nuclear magnetic resonance relaxometry were used to study molecular and collective dynamics in unilamellar liposome systems. Relaxation data for liposomes of diameter about 100 nm composed of 1,2-dimyristoyl-*sn*-glycero-3-posphocholine (DMPC) or 1,2-dioleoyl-*sn*-glycero-3-posphocholine (DOPC) were obtained. The Larmor frequency dependence of the spin−lattice relaxation rates was interpreted in terms of clearly defined relaxation mechanisms associated with the underlying molecular dynamics. The physical parameters obtained from the analysis are consistent with values available in the literature obtained from a range of experimental techniques. This work establishes the potential of our approach to study dynamics in liposomal samples of more complex lipid composition.

Introduction

Lipid dynamics in biological membranes has been a subject of enormous interest to the scientific community over a great many years.[1] This is in part because the viscoelastic and hydrodynamic properties of membranes, which are critical in determining their function as selective permeability barriers, arise from interactions that occur on the molecular length scale and over the time scale for molecular dynamics.[2] It is also increasingly apparent that critical molecular events, such as the action of membrane-bound proteins, are inherently linked with the surrounding lipid environment. Thus, cholesterol-rich membrane "rafts" have been identified as the site of action of a wide range of membrane-bound proteins,[3,4] and the properties of these domains have been extensively studied.[5,6] Aqueous lipid bilayer vesicles, often referred to as liposomes, can be prepared by dispersing synthetic or natural phospholipids in excess water. Liposomes resemble cell membranes in structure and composition and are an excellent model for studying membrane function and dynamics. The biomedical applications of liposomes, usually for the delivery of therapeutic or diagnostic agents, are critically dependent on the microscopic molecular interactions within the membranes, which determine permeability, release rate, vesicle size, and stability.

As insights gained from physicochemical characterization of dynamics in lipid membranes are of relevance to cell biology and bionanotechnology, a wide range of experimental methods have been applied to their study.[7] This is necessary as dynamic processes in lipid membranes occur over a broad range of time scales, with associated correlation times ranging from 10^{-15} s, for molecular vibrations, to hours for the lipid flip-flop process.[8] Among the most commonly used methods is nuclear magnetic resonance (NMR), as it is sensitive to dynamics over a very broad time scale. Other techniques that have been applied include Raman and infrared spectroscopy, electron paramagnetic resonance (EPR), fluorescence correlation spectroscopy (FCS), fluorescence recovery after photobleaching (FRAP), X-ray spectroscopy, and neutron scattering.

NMR studies of biological and model membranes were first reported in the early 1970s.[9−13] At ^{1}H Larmor frequencies in the conventional megahertz range, various types of noncollective motions associated with local molecular reorientations dominate and tend to mask the collective dynamics. The first field-cycling NMR relaxometry studies in lipid membranes were reported almost 30 years ago.[14,15] In this technique, the magnetic field, and hence Larmor frequency, dependence of the spin−lattice relaxation in the laboratory frame is measured. By applying a theoretical framework, this approach allowed the authors to obtain information on the underlying motions driving the spin relaxation at a given temperature. A division between high frequency individual and low frequency collective motions was noted, for the liquid crystalline phase of both 1,2-dipalmitoyl- and 1,2-dimyristoyl-*sn*-glycero-3-phosphocholine, known as DPPC and DMPC, respectively. At lower temperature, in the gel phase, the collective motions were found to be suppressed.

The Larmor frequency dependence of the spin−lattice relaxation time (T_1) in planar bilayer membranes, arising due to membrane "undulations", was discussed by Marqusee.[16] Time scale separation arguments were applied, and so cross-correlations between contributions from fast motions and slow motions associated with collective order fluctuations were omitted. A linear frequency dependence of T_1 was predicted for the slower motions, a result which is similar to other models for smectic thermotropic liquid crystals. This result was later used to explain the proton T_1 dispersion, as measured using the fast field-cycling (FFC) technique, in multilamellar vesicles (MLVs) of DMPC.[17] MLVs are composed of a variable number of concentric lipid bilayers. The study revealed the presence of a strong T_1 dispersion in the low-frequency regime, which was interpreted in terms of cooperative smectic-like motions. The approach used required a large number of motional types to be included for successful fitting: order fluctuations, molecular rotations, lateral

* Corresponding authors. E-mail: dermot.brougham@dcu.ie; anoardo@famaf.unc.edu.ar.
[†] Dublin City University.
[‡] CONICET.

10.1021/jp907084s CCC: $40.75
Published on Web 11/03/2009

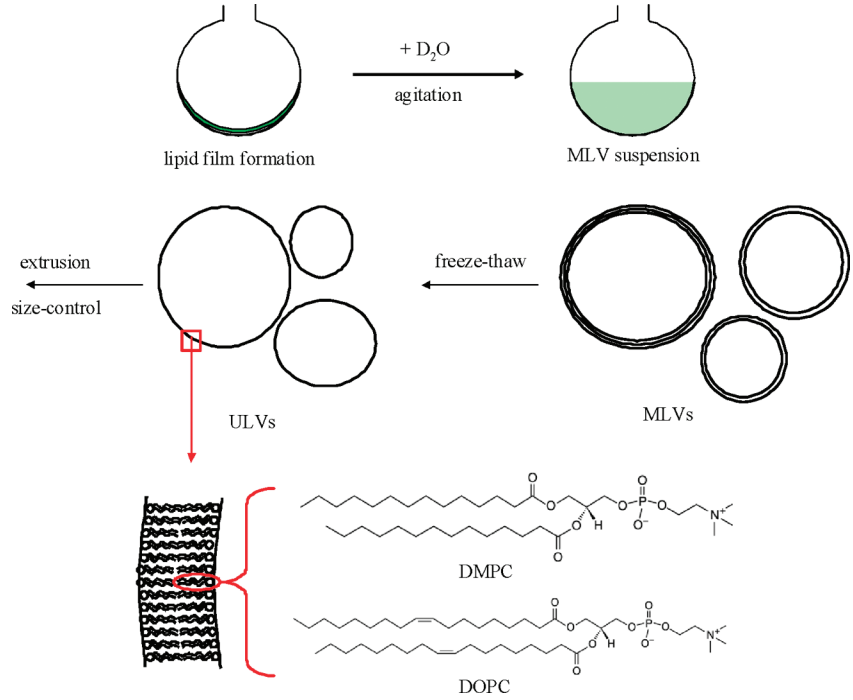

Figure 1. Schematic representation of the formation of unilamellar and multilamellar vesicles, LUVs and MLVs, respectively. The molecular structures of 1,2-dimyristoyl-*sn*-glycero-3-phosphocholine (DMPC) and 1,2-dioleoyl-*sn*-glycero-3-phosphocholine (DOPC) are included.

diffusion, and translationally induced rotations due to motion over a curved surface, all of which were considered as statistically independent and were modeled with a large number of free parameters. This approach is susceptible to overinterpretation and possible bias.[18] It should also be noted that the possibility of coupling of motions between the lipid layers may be a complicating factor for MLVs, not present in cell membranes or drug carrier systems. A linear dispersion for T_1 was also predicted by considering shape fluctuations of vesicles when interlayer interactions are neglected, which would be the case for large unilamellar vesicles (LUVs).[19]

The Larmor frequency dependence of the spin−lattice relaxation due to diffusion on curved surfaces was subsequently considered by Halle.[20] For isotropic micellar solutions, the model reduced to a Lorentzian spectral density. It has been suggested that translational diffusion is too slow to contribute within the kilohertz frequency range in vesicles larger than a few hundred nanometers.[19] The applicability of this assumption to smectic lipid bilayers is one of the subjects that we will address in this work.

An alternative to relaxation dispersion analysis in terms of the involved dynamical mechanisms is to use a model-free approach, in which case the number of spectral density components included is determined by a merit function, or other statistical analysis, of the data. Both the Lipari−Szabo[21] and King−Jardetzky[22] approaches utilize a sum of Lorentzians or modified functions which are appropriate for interpreting the relaxation dispersions of protein solutions. It is clear, however, that this will cause difficulties in reproducing dynamical processes demanding a description in terms of a broad distribution of correlation times, like collective order fluctuations.

In this paper, we present a consistent interpretation of the ^{1}H T_1 relaxation dispersion in DMPC and DOPC (1,2-dioleoyl-*sn*-glycero-3-phosphocholine) LUVs, prepared in excess deuterated water (see Figure 1). Phosphatidylcholine is the most abundant lipid class in most biological membranes,[1] and it is easily available, is biologically relevant, and has optimal physicochemical properties. There is significant literature describing the preparation, characterization, and applications of phosphatidylcholine vesicles, particularly those composed of DMPC and DOPC. Hence, LUVs formed using these synthetic lipids are excellent model systems for the evaluation of new approaches to studying dynamics in membranes, which are not affected by the potential complication of interlayer coupling, as would be the case for MLVs. As our intention was to make comparisons between the results for the two types of lipid, extrusion was used to ensure that the average hydrodynamic diameter of the samples was the same, c. 100 nm. The aim of the study is to establish whether the relaxation dispersions can be interpreted quantitatively using models for well-known membrane dynamical processes on the molecular scale.

Experimental Section

Reagents. 1,2-Dioleoyl-*sn*-glycero-3-phosphocholine (DOPC) and 1,2-dimyristoyl-*sn*-glycero-3-phosphocholine (DMPC) were purchased as lyophilized powders (>99%) from Avanti Polar Lipids (Alabaster, AL) and stored at −20 °C. Deuterium oxide (D_2O, purity 99.9%) was obtained from Apollo Scientific Limited (UK). All reagents were used without further purification.

Liposome Preparation. Uniform mixtures of phospholipid and cholesterol were prepared by dissolving ∼70 mg of DOPC, or DMPC, in 2 mL of $CHCl_3$. The solvent was removed under a slow stream of N_2 over 24 h. Liposomes were prepared by hydrating the mixtures in 1.5 mL of deuterium oxide (5 M proton, 0.06 M lipid) under a constant flow of Ar. The suspensions were heated above T_m to ∼22 °C for DOPC and ∼35 °C for DMPC for 24 h, followed by three heating/cooling/shaking cycles to ensure a homogeneous preparation. Following hydration, the vesicle solutions were exposed to six freeze−thaw cycles using liquid N_2 and warm water (40 °C), then passed through an Avanti Polar Lipids mini extruder (Alabaster, AL) containing polycarbonate membranes with a pore size of 0.2 or 0.1 μm (Whatman Nuclepore; Clifton, NJ). The extrusion

process was carried out above T_m in an AtmosBag glovebag (Aldrich Chemical Co.; Milwaukee, WI).

Dynamic Light Scattering. The average sizes of the unilamellar liposome suspensions were determined using a High Performance Particle Sizer HPPS (Malvern Instruments, Malvern, UK) using a detection angle of 173° and a 3 mW He−Ne laser operating at a wavelength of 633 nm. The mean hydrodynamic diameter is based upon the intensity of scattered light.

Relaxation Rate Dispersion Experiments. ^{1}H relaxation rate dispersions (also termed NMRD dispersions) were measured using the fast field-cycling NMR technique[23] with a Spinmaster FFC-2000 Fast Field Cycling NMR Relaxometer (Stelar, Mede, Italy) for liposome samples of 1 mL volume. In all cases a polarization magnetic field of 0.329 T (equivalent to 14 MHz for ^{1}H) was used, which was switched on for a period of 0.5 s to generate sample magnetization. The value of the acquisition field was 0.217 T (9.25 MHz). A field slew rate of 0.47 T·ms^{-1} (20 MHz·ms^{-1}) was used in all cases, with a switching time of 1.5 ms to allow the magnetic field to settle. A digitization rate of 1 MHz was used for acquisition, while the dead time of the spectrometer was about 20 μs. The FID was sampled with 512 points in the time range 25−540 μs, after the front edge of the 90° pulse, which was of 7.5 μs duration.

The relaxation rates, R_1, were determined from the magnetization recovery curves by least-squares fitting. The R_1 values were not sensitive to the time window over which the FID was sampled. The spin relaxation process for all samples was found to be monoexponential, within error, at all frequencies. The sample temperature was controlled to within about 0.5 K using the Spinmaster Variable Temperature Controller. Temperatures were calibrated externally using a Cu−Al thermocouple in a 10 mm NMR tube. The time for each experiment is limited by the stability of the suspensions, and after several days changes were observed in both T_1 and the hydrodymanic size. For the data presented, there were typically 64 repeat scans at each frequency, and the total measurement time was c. 24 h, during which time the suspensions were unchanged.

Measurement of the Local Field. The fixed-lock relaxation technique in the rotating frame was used to estimate the average residual component of the local fields (B_L) along the main quantization axis.[24] This value is needed to correct the effective low-range Larmor frequency sensed by the spins and to decide the minimum frequency from which the relaxation data can be considered free of undesirable local field effects. The rotating frame frequency was scanned from 6 to 40 kHz. The $\pi/2$ pulse length was 2.6 μs at a working Larmor frequency of 19.181 MHz. The apparatus is based on a Stelar Spinmaster console and a Bruker BE10 electromagnet. The probe was adapted to a Kalmus LP-1000 power transmitter. A sample temperature was directly measured in the sample volume within ±1 K with a CHY 503 digital thermometer. The intensity of the FID signal was measured as a function of the lock-field amplitude B_1 at a fixed lock-time of $\tau = 5$ ms.

Results

Local Field in LUV Suspensions. Experimental data obtained using the fixed-lock relaxation technique and the corresponding fitting function are plotted in Figure 2, clearly showing that the magnetization decays when the applied lock-field is reduced in intensity. The evolution of the magnetization for an on-resonance spin-lock in the presence of a local field can be approximated by[24]

$$M(\nu_1) = \frac{M_0}{1 + \left(\frac{B_L}{B_1}\right)} \exp\left\{-\frac{\tau}{B_L^2 + B_1^2}\left[\frac{B_1^2}{T_b} + \frac{B_L^2}{T_D \exp\left(\frac{B_1^2}{B_L^2}\right)}\right]\right\}$$

Here, M_0 is the initial magnetization (normalized to 1); B_1 is the amplitude of the lock-field (and $\nu_1 = \gamma B_1$ is the rotating-frame Larmor frequency); T_D is a dipolar relaxation time; T_b is the spin−lattice relaxation time along the $\boldsymbol{B_1}$ field, which is equivalent to $T_{1\rho}$ (the spin−lattice relaxation time in the rotating frame) far from the local field region (a value of 20 ms was measured at 20 kHz). T_D was assumed to be of the same order as T_b.[25] With these conditions, we obtain B_L values (in ^{1}H Larmor frequency units) of (12 ± 1) kHz and (11 ± 1) kHz for DMPC and DOPC, respectively (see solid line in Figure 2). The evolution of the magnetization at frequencies comparable to, or lower than, the local field may be influenced by processes other than spin−lattice relaxation. Therefore, measurement of the spin−lattice relaxation rate, $R_1 = T_1^{-1}$, should be limited to frequencies in excess of B_L.

^{1}H Spin−Lattice Relaxation in LUVs. DOPC and DMPC LUV suspensions with vesicle diameter of about 100 nm were prepared by extrusion, to facilitate comparison of the relaxation dispersions of suspensions of both types of lipid. To ensure that the lipids were in the fluid, liquid crystalline phase, measurements should be performed at least 10 K above the main phase transition temperature (T_m) of the lipid, which occurs at ∼297 and ∼255 K for DMPC and DOPC, respectively.[26] Thus, measurement temperatures of 310 and 298 K were chosen for DMPC and DOPC, respectively. In forthcoming work, the size and temperature dependence of the ^{1}H relaxation dispersions for LUVs will be presented. Our aim here is to establish experimental and analysis methodologies for liposomes of different composition.

Figure 3 shows the relaxation rate dispersions of DOPC and DMPC LUVs obtained by the field-cycling method in the frequency range from 30 kHz to 15.2 MHz, where we can be

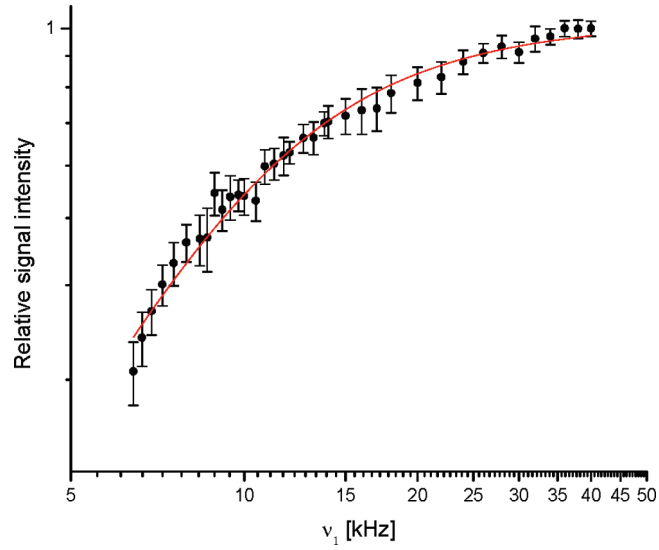

Figure 2. Normalized magnetization as a function of ν_1 at a fixed lock-time $\tau = 5$ ms for a DMPC suspension. The decay of the sample magnetization as the lock field amplitude is reduced is a consequence of residual local fields. The average local field component along the laboratory-frame quantization axis can be determined as described in the text. Error bars correspond to data dispersion after 10 repetitions at each frequency.

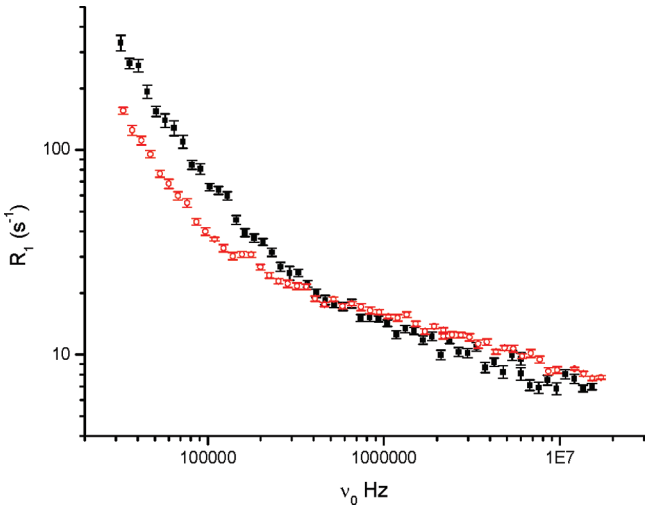

Figure 3. ^{1}H relaxation rate dispersion data, recorded above T_m (see text), for a DMPC LUV suspension of average $R_0 = 54$ nm (red ○) at 310 K and for a DOPC suspension of average $R_0 = 50$ nm (■) at 298 K. The error bars are estimates of the random errors obtained from least-squares fitting of the ^{1}H magnetization recovery curves.

confident that we are measuring R_1 without spurious effects from local fields. It is immediately clear from Figure 3 that the frequency dependence of the relaxation rate is complex and that it cannot be modeled using a single Lorentzian function, which would correspond to a single random stochastic dynamic process. There is also an apparent increase in slope in the range slightly less than 1 MHz, indicating a change in the relaxation mechanism below this frequency. This is particularly apparent for the DOPC suspension.

Discussion

1. Contributing Relaxation Mechanisms in LUVs. Any relaxation theory relates the measured relaxation times to the microscopic properties of the sample. We will consider the frequency interval where the conditions of the weak collision limit of the semiclassical approach are valid. In this limit, fluctuations are intense during the time scale of the relaxation process, even before it has perceptible influence on the spin system. In this formalism, the relaxation times are represented through spectral density functions that model the lattice dynamics. In turn, the spectral densities are the Fourier transforms of the corresponding correlation functions. The latter contain the relevant physics of the problem thus relating the measured times with the involved physical parameters (viscosity, elastic constants, etc.) and the externally controlled variables (temperature, frequency, orientation, etc.). In the absence of paramagnetic species, fluctuations of the homonuclear dipolar interaction are considered to be the dominant relaxation mechanism for ^{1}H nuclei. Within this picture, the spin−lattice relaxation time for an orientationally averaged sample can be expressed as[27]

$$\frac{1}{T_1} = K[J_1(\omega) + 4J_2(2\omega)] \qquad (1)$$

where $K = (9/8r^6)\gamma^4\hbar^2(\mu_0/4\pi)^2$; r is the mean interproton distance; γ is the proton magnetogyric ratio; $\hbar$ is Plank's constant divided by 2π; and μ_0 the vacuum magnetic permeability. Finally, $\omega = 2\pi(\nu_0 + \nu_L)$, where ν_0 is the magnetic field in ^{1}H Larmor frequency units and ν_L is the offset field due to the average local field component along the quantization axis. The normal component correction is less relevant, so in this work we will only consider data for magnetic fields well in excess of the local field magnitude B_L.

In eq 1, the spectral densities correspond to the Fourier transform of the resulting correlation functions including all the dynamics of the system. It is commonly assumed that the different contributing mechanisms are statistically independent, in which case the system correlation function will be reduced to the product of the correlation functions of the individual motions. Time scale separation is also frequently invoked allowing reduction of the product to a sum, and hence the total spectral density can be reduced to the sum of spectral densities from the independent contributing motions.[16,17] For a given complex dynamic system, the assumption that there is no cross-correlation between different processes must be validated.[28]

In the following discussion, we will consider the relevant dynamical processes that are accepted as being present in lipid membranes and the physical models that can be applied to study them. Our strategy, aimed at minimizing the risk of overinterpretation, is based on applying the results of independent experiments, where possible. Later, at the time of selecting an adequate physical model, boundary conditions and approximations are considered. Flip-flop jumps of lipid molecules may occur with characteristic times ranging from hours to days,[8,29] so will not be considered.

Order Fluctuations. Quasi-spherical fluctuations[30] in unilamellar vesicles are well established as the main order fluctuation mechanism through transverse nuclear spin relaxation studies.[31,32] The corresponding spectral density was calculated by M. Vilfan et al. in the limit of slight deformations.[19] The vesicle is considered as a flaccid quasi-spherical shell of radius R_0 with constant volume $V = (4/3)\pi R_0^3$ and fixed area A. For a quantitative description, the deformed spherical surface can be represented as

$$R(\theta,\phi) = R_0[1 + u(\theta,\phi)] \qquad (2)$$

where $u(\theta,\phi)$ represents the instantaneous displacement of the vesicle surface from its spherical conformation in terms of the polar and azimuthal angles defining the position on the sphere. $u(\theta,\phi)$ can conveniently be expanded in terms of spherical harmonics representing the discrete normal modes. By analogy with the case of liquid crystals, the corresponding correlation function can be defined in terms of the components of a unit vector $\mathbf{n} = (n_r, n_\theta, n_\phi)$ representing the instantaneous direction of the local membrane normal. In the small angle approximation we have

$$J_{OF}(\omega) = \mathrm{Re}\int_{-\infty}^{\infty}[\langle n_\theta(0)n_\theta^*(t)\rangle + \langle n_\phi(0)n_\phi^*(t)\rangle]e^{-i\omega t}\mathrm{d}t \qquad (3)$$

For small fluctuations, the components of the unit vector and the instantaneous displacement are related by

$$n_\theta = -\frac{\partial u(\theta,\phi)}{\partial\theta} \qquad n_\phi = \frac{-1}{\sin\theta}\frac{\partial u(\theta,\phi)}{\partial\phi} \qquad (4)$$

Therefore, we obtain the spectral density as a sum of contributions of individual excitation modes characterized by the number l (the same index as is used for spherical harmonics), ranging from the minimum mode contributing to relaxation ($l = 2$) to a maximum value determined by the

molecular dimensions ($l_{max} \approx \pi R_0/a$, where a is the average distance between neighboring molecules)

$$J_{OF}(\omega) = \frac{k_B T}{2\pi\kappa} \sum_{l=2}^{l_{max}} \frac{l(l+1)(2l+1)}{(l^2+l-2)(l^2+l+\sigma)} \frac{\tau_l}{(1+\omega^2\tau_l^2)} \quad (5)$$

Here, κ is the bending elastic modulus; k_B is the Boltzmann constant; T is the temperature; σ is the effective lateral tension; and τ_l is given by

$$\tau_l = \frac{\eta R_0^3}{\kappa} \frac{(2l+1)(2l^2+2l-1)}{l(l+1)(l+2)(l-1)(l^2+l+\sigma)} \quad (6)$$

where η is the viscosity of the supporting fluid. On a logarithmic scale, the model results in a linear frequency dependence over a wide frequency range, with a low-frequency plateau, the value of which depends on R_0, η, κ, and σ.[19] The magnitude of R_1 is independent of the size of the vesicle, and when the radius is increased, the linear regime covers a wider frequency range; this is as expected as the membrane of a larger vesicle will have reduced curvature.

Diffusion on a Curved Surface (Small Liposomes). Diffusion coefficients as high as 10^{-11} m^2 s^{-1} were reported for phospholipid molecules in the liquid-crystalline phase of model membranes.[33−35] It is well established that diffusion is an important dynamical process taking place on curved membrane systems. In the present context, the theory proposed by Halle for spin relaxation due to diffusion on curved surfaces is appropriate,[20] provided that the liposomes can be modeled as spheroids. This approach assumes that the suspension is diluted sufficiently to prevent direct interaction between liposomes. In our case, the volume fraction of liposomes in the samples can be as high as 10%, so direct interactions between liposomes certainly occur. The fact that the average liposome size remains stable for several days demonstrates that the interactions are weak. However, in any case such interactions would only modify the reorientational properties of the entire sphere. The fluctuation of the spin−lattice coupling is considered to have two different contributions: the translational motion of the molecules along the spheroidal surface and the reorientation of the sphere as a whole. Provided that each event occurs on a different spatial scale, it is reasonable to assume that the two processes are statistically independent. In the case of isotropic micellar solutions, the model reduces to a Lorentzian function

$$J_D(\omega) = \frac{1}{5}\left[\frac{\tau_D}{1+(\omega\tau_D)^2} + 4\frac{\tau_D}{1+(2\omega\tau_D)^2}\right] \quad (7)$$

where τ_D is the joint correlation time related to the rotational-diffusion correlation time, τ_{RD}, and the surface-diffusion correlation time, τ_{TD}, by

$$\frac{1}{\tau_D} = \frac{1}{\tau_{RD}} + \frac{1}{\tau_{TD}} \quad (8)$$

with

$$\tau_{RD} = \frac{4\pi\eta R_0^3}{3k_B T} \qquad \tau_{TD} = \frac{R_0^2}{6D} \quad (9)$$

and D is the translational molecular diffusion coefficient. The diffusion coefficient can be estimated from the classical analysis of Brownian motion within the hydrodynamic regime.[36] In this model, the membrane is considered to be an infinite planar sheet of fluid with a given viscosity (lipid layer) separated by infinite regions of lower viscosity (supporting fluid). The lipid is regarded as a cylinder whose axis is perpendicular to the plane of the sheet, moving under the action of Brownian motion.

Fast Motions. The third relevant relaxation mechanism that has to be considered is the fast motions of individual molecules or internal parts of them. Within this group, we can mention internal vibrational fluctuations, librations, isomerizations, rotations of small chemical groups, hydrocarbon chain fluctuations, etc. The correlation times associated with these processes range typically from 10^{-10} to 10^{-12} s, thus becoming dispersive at frequencies greater than several megahertz. It is not possible to discriminate between these mechanisms within the studied frequency range (a few kilohertz to 20 MHz). They add a frequency-independent contribution represented by a constant, A_{FM}.

Composite Spectral Density. As the amplitude of fast motions of stochastic nature is generally small, they can be considered statistically independent from the dynamics governing relaxation at low fields. The rate of decay of the correlation function for fast motions, $G_{FM}(t)$, is much faster than for order fluctuations and slow diffusion; thus the fast motions can be considered separately, without risking underestimation of cross-correlation terms. In principle, order fluctuations and diffusion are coupled, as the diffusing molecule transports information regarding local order orientation. While the evaluation of a cross-correlation term is beyond the scope of the present work, we can instead simplify the situation by considering the following two arguments:

(i) A practical consideration that must be borne in mind is that the transport of "order information" is restricted, as the diffusional random walk of the lipid molecules is limited to a small area. Specifically, in 100 ns, the area traversed by the diffusing lipid is only 3 times the average cross-sectional area of a single lipid.[37] Order information will only be preserved by the lipid molecules for a maximum time determined by the longest correlation time corresponding to $l = 2$; typically, this corresponds to $\tau_{l=2} \approx 3$ μs. In this time, the area traveled by a lipid molecule is <100 molecular cross sections, an area much too small for a useful exchange of order information between regions of different membrane curvature.

(ii) Taking a different perspective, we can generalize the calculation of Freed corresponding to a cross-correlation between nematic order fluctuations and a Lorentzian process.[28] In that case, there is a minimum wavelength for the propagating perturbation, which is associated with the molecular dimensions. Hence the associated cutoff frequency, ω_c, is in the megahertz range. Extending Freed's result to smectic order fluctuations within the range $\omega \ll \omega_c$, we can approximate the composite spectral density as

$$J(\omega) \approx A_D J_D(\omega) + A_{OF} J_{OF}(\omega)\left\{1 - \alpha\left(\frac{\omega}{\omega_c}\right)\left[1 + \frac{\tau_D}{1+(\omega\tau_D)^2}\right]\right\} \quad (10)$$

where $A_{OF} \approx A_D$ are the corresponding amplitude prefactors (see eq 1). For $\omega_c \approx 10^9$ Hz, it can be verified that

$$\alpha\left(\frac{\omega}{\omega_c}\right)\left[1 + \frac{\tau_D\omega_c}{1 + (\omega\tau_D)^2}\right] \ll 1 \qquad (11)$$

holds valid for ω in the range of 10^4-10^7 rad·s^{-1} with $\tau_D \approx 10^{-5}$ s. So, to a first approximation, we can ignore cross-correlation between the diffusional and collective dynamics contributions.

Finally, in this simple model, the relaxation rate, R_1, can be expressed as

$$R_1 = \frac{1}{T_1} = A_{OF}J_{OF}(\omega) + A_DJ_D(\omega) + A_{FM} \qquad (12)$$

where $J_{OF}(\omega)$ is given by eq 5 and eq 6; $J_D(\omega)$ is given by eqs 7−9; and A_{FM} is a constant.

2. Interpretation of the Relaxation Rate Dispersions. We have adopted the following systematic approach to simulating the ^{1}H relaxation dispersions of LUVs:

(i) Identify the motions that contribute and assign appropriate spectral density functions.

(ii) Fix the relevant physical parameters within their most probable intervals, using the literature values. This is the main reason that we have concentrated on DMPC and DOPC LUVs, as the properties of bilayers formed from these lipids are very well characterized.

(iii) Set the frequency-independent contribution (a constant) and select the optimal parameter set within their most probable intervals, to reproduce the experimental relaxation rate dispersion.

(iv) Make fine adjustments to the amplitudes (prefactors) of each spectral density contribution, if required (see eq 12). This was done manually by observing the effect of minor adjustments on the agreement between the simulation and experimental data.

The prefactors are largely determined by the effective interproton distances, arising from the usual inverse sixth-power dependence. In all cases, the prefactors used correspond to effective interproton distances ranging from 2.6 to 4.7 Å. However, at this stage our aim is not to use the data to obtain structural information but rather to concentrate on establishing the number and form of the spectral density contributions that are required to interpret the data, i.e., to establish the viability of the methodology. Application of our approach to extract physical information for LUV suspensions, which will be the subject of forthcoming work, will only be possible after the model is tested in different circumstances.

The result of this approach to the interpretation of the ^{1}H relaxation dispersion of a DMPC LUV suspension is presented in Figure 4. The model parameters corresponding to the simulated relaxation dispersion curve are given in Table 1. Errors in each quantity were determined by analyzing the sensitivity of the simulated curve to variations of each parameter. The error interval corresponds to a maximum shift of the simulation curve within the experimental error (approximately the size of data points). It is very important to note that it is not possible to produce the reasonable agreement with the experimental relaxation dispersion shown, without including the low-frequency Lorentzian contribution.

It is clear from Figure 4 that the simple model underestimates R_1 in the low megahertz range, specifically between 600 kHz and 3 MHz. This suggests that an additional dynamical process, effective within that frequency range, should be considered. In other words, a further iteration of the systematic approach to the simulation, described in steps (i) to (iv) above, is required. Assuming a Lorentzian contribution, the associated correlation time would be of the order of 10^{-6} to 10^{-8} s. An assumption of the simple model is that all motions other than order fluctuations and diffusion are too fast to contribute to the dispersion in the accessible frequency range. This approach was adopted to test the applicability of the simplest possible spectral density function and to avoid overinterpretation of the data. It is now apparent that the data require a contribution, from a dynamic process operating on this time scale, to the total spectral density.

It is most probable that this process is associated with slow molecular dynamics; correlation times, τ_c, in the range 10^{-7} to 10^{-10} s have been suggested for chain isomerization or molecular rotation along the long axis and have been shown to affect the ^{1}H and ^{2}H line-width.[43] More recently, molecular dynamics simulations and high-frequency ^{2}H and ^{13}C relaxometry were used to determine the rotational diffusion of the entire lipid, suggesting τ_c values in the 10^{-7} to 10^{-8} s range.[44] Thus, there is precedent for relaxation contributions in this frequency range, and so an additional Lorentzian term should be added to the total spectral density. Since fast motions are the main contributing mechanism at frequencies higher than 600 kHz, statistical

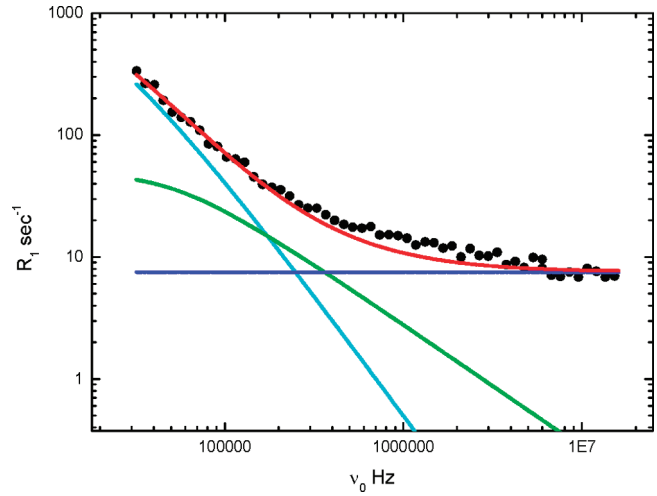

Figure 4. Experimental relaxation dispersion for a DMPC LUV suspension, average $R_0 = 54$ nm, at 310 K (experimental data points in black). The simulated dispersion curve is shown in red. Contributions from each type of motion are included: order fluctuations (green), diffusion (cyan), and fast motions (blue). See parameters in Table 1. It can be observed that around 1 MHz the model underestimates R_1, suggesting that a contributing mechanism, relevant within this range, is absent from our interpretation.

TABLE 1: Parameters Corresponding to the Simulated Spectral Density Contributions to the DMPC Relaxation Dispersion Depicted in Figure 4 and Corresponding References

parameter	model value	range[a]	references
η [kg/s·m]	0.83×10^{-3}	$(0.8 - 0.9) \times 10^{-3}$	30, 38
σ	0	0−25	19, 30, 34
a [nm]	1	1−1.2	31, 36, 39
κ [J]	$(3.1 \pm 0.6) \times 10^{-20}$	4×10^{-21}−4.2×10^{-19}	30, 40
A_{OF} [s^{-2}]	$(7.5 \pm 1.8) \times 10^8$	1.6×10^7−6.4×10^{10}	15, 41
A_D [s^{-2}]	$(2.1 \pm 0.6) \times 10^9$	1.6×10^7−6.4×10^{10}	15, 41
D [m^2 s^{-1}]	$(0.8 \pm 0.2) \times 10^{-11}$	10^{-12}−10^{-10}	36, 37, 42
A_{FM} [s^{-1}]	7.5 ± 1.3	not applicable	-

[a] Range within which there are reported experimental values from other techniques.

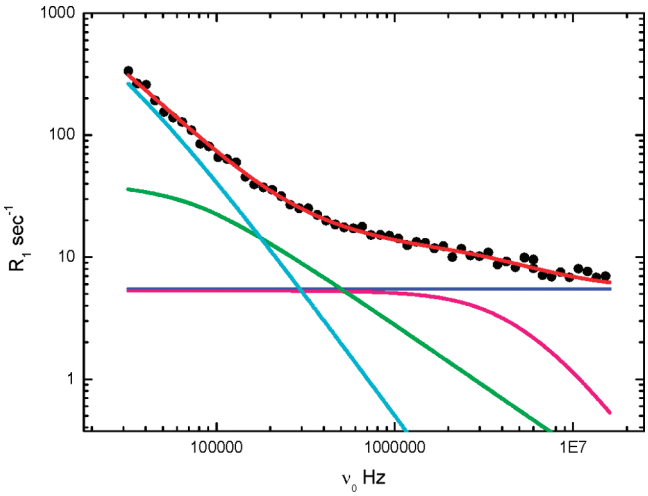

Figure 5. Experimental relaxation dispersion for a DMPC LUV suspension, average $R_0 = 54$ nm, at 310 K. The simulated dispersion curve including correction is shown in red (see text). A new Lorentzian contribution associated with rotational diffusion of lipid molecules is included (pink), with $\tau_R = (1.8 \pm 1.7) \times 10^{-8}$ s and $A_R = (0.6 \pm 0.1) \times 10^8$ s^{-2}. The other contributions are the same as shown in Figure 4, with parameters unchanged from the previous simulation, given in Table 1, with the exception of the frequency-independent contribution that is now reduced to $A_{FM} = (5.5 \pm 1.3)$ s^{-1}.

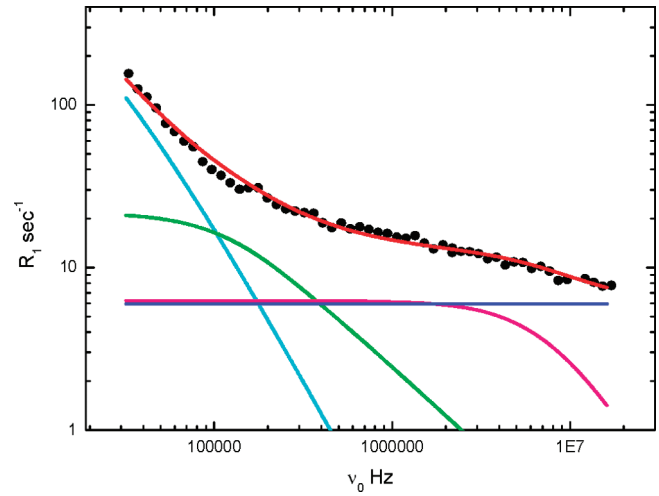

Figure 6. Experimental relaxation dispersion for a DOPC LUV suspension, average $R_0 = 50$ nm, at 298 K. The simulated curve is shown in red. Contributing mechanisms are the same as shown in Figures 4 and 5. All parameters used are given in Table 2.

TABLE 2: Parameters Corresponding to the Simulated Spectral Density Contributions to the DOPC Relaxation Dispersion Depicted in Figure [6] and Corresponding References

parameter	model value	range	references
η [kg/s·m]	1.1×10^{-3}	$(0.8 - 0.9) \times 10^{-3}$	38, 30
σ	0	0−25	19, 30, 34
a [nm]	1	1−1.2	36, 31, 39
κ [J]	$(5.4 \pm 0.9) \times 10^{-20}$	4×10^{-21}−10^{-19}	40, 45, 46
A_{OF} [s^{-2}]	$(1.18 \pm 0.28) \times 10^9$	1.6×10^7−0.4×10^{10}	15, 41
A_D [s^{-2}]	$(1.50 \pm 0.25) \times 10^9$	1.6×10^7−0.4×10^{10}	15, 41
D [m^2 s^{-1}]	$(0.3 \pm 0.2) \times 10^{-11}$	10^{-10}−10^{-12}	47, 48, 5, 49
A_R [s^{-2}]	$(1.1 \pm 0.4) \times 10^8$	1.6×10^7−0.4×10^{10}	15, 41
τ_R [s]	$(1.1 \pm 0.3) \times 10^{-8}$	10^{-10}−10^{-7}	43, 17, 44
A_{FM} [s^{-1}]	6 ± 1	not applicable	

independence and time scale separation arguments can again be evoked. Equation 12 then becomes

$$\frac{1}{T_1} = A_{OF}J_{OF}(\omega) + A_DJ_D(\omega) + A_RJ_R(\omega) + A_{FM} \tag{13}$$

where A_R is the rotational amplitude factor and the spectral density $J_R(\omega)$ has the same form as eq 7, but with τ_D now replaced by the rotational correlation time τ_R.

The addition of this Lorentzian spectral density contribution (with a correlation time $\tau_R = (1.8 \pm 1.7) \times 10^{-8}$ s and amplitude $A_R = (0.6 \pm 0.1) \times 10^8$ s^{-2}) improves the simulated dispersion (see Figure 5). So the simulation reproduces the experimental R_1 curve, within error, without any change in any of the other parameters, except for a slight adjustment in the frequency independent term, which was reduced to $A_{FM} = (5.5 \pm 1.3)$ s^{-1}. This result suggests that a contribution from a motion on the expected time scale for molecular rotational is indeed efficient around 1 MHz and cannot be neglected.

The same systematic approach was applied to simulate the relaxation dispersion of DOPC. Again the inclusion of a molecular rotational diffusion term was required to obtain a satisfactory agreement with the experimental data (see Figure 6). The corresponding parameters are given in Table 2.

3. Evaluation of the Analysis. The good agreement between simulation and the experimental relaxation dispersions for both DMPC and DOPC is very encouraging. It is important to emphasize that the present analysis provides no further insight into the differences in dynamics between DMPC and DOPC lipid bilayers; the published values for the physical parameters of these membranes are sufficient to reproduce the experimental LUV ^{1}H relaxation dispersions.

A closer examination of the numerical values that produced the simulations in Figures 5 and 6 reveals trends in the parameters for lipid molecular motions for DOPC and DMPC that are in broad agreement with expectation. For instance, the unsaturation present in DOPC is known to disrupt the chain packing, resulting in an increase in the average interfacial area per lipid; values of 59.6 and 72.5 Å^2 have been reported for DMPC and DOPC, respectively.[50] This reportedly results in an increase in rate of rotational motion of the phospholipid molecules[51] consistent with a reduction in the correlation time. The τ_R values of 1.83×10^{-8} and 1.09×10^{-8} s used in our simulations for DMPC at 310 K and DOPC at 298 K, respectively, are consistent with this trend. In the case of diffusion, pulsed-field-gradient NMR measurements of the diffusion coefficient of lipids in macroscopically aligned layers have also been performed.[5] D_{PFG} values of $\approx 12 \times 10^{-12}$ m^2 s^{-1} can be inferred for DMPC at 310 K (from PFG measurements at 308 and 313 K), and a D_{PFG} value of 8×10^{-12} m^2 s^{-1} at 298 K was reported for DOPC. While the values for the diffusion coefficients utilized in our simulations are somewhat lower (8×10^{-12} and 3×10^{-12} m^2 s^{-1}, for DMPC and DOPC, respectively), they are within the literature ranges[5,36,37,42,47−49] and they appear to show the same trend reported by Filippov et al.[5]

Looking at the high frequency part of the relaxation rate dispersions, the exact nature of the dynamic contribution we have described as "rotational" remains to be ascertained. The Lorentzian form of the spectral density function successfully applied suggests that this is a stochastic process on the time scale of $1-2 \times 10^{-8}$ s for DOPC and DMPC LUVs. Further insight into the nature of this process is difficult to obtain from relaxometry, and we can only note that the average ^{1}H−^{1}H

interatomic distance for the dipolar interactions that modulate the spectral density is ~3.6 Å. Finally, our results confirm that there are fast motions that contribute equally to the relaxation rate across the accessible frequency range.

We have also considered other approaches to interpreting the relaxation data, including the model-free approach.[18,21,22] This approach produces comparably good agreement with the data but necessitates the inclusion of a large number of free parameters, i.e., an effective correlation time and a prefactor for every Lorentzian spectral density contribution required to fit the data. However, it does present significant difficulties: (i) Relating the τ_c values to the physical properties of the membranes is nontrivial. (ii) The description of the collective dynamics in terms of Lorentzian functions is problematic. (iii) The number of contributions required to fit the data is very sensitive to the data range, and in our experiences it is also sensitive to small changes in average hydrodynamic size and temperature. We conclude that the approach described here is more robust, and potentially more useful, for the interpretation of LUV relaxation data.

We also undertook a series of experiments on MLV suspensions of both DMPC and DOPC. We found that the measured T_1 values were always longer for MLV suspensions but that the suspensions were far less stable. The light scattering and NMR responses were observed to change significantly over several hours, as the sample aged. Given the impossibility of size control for this type of suspension, the potential for interlayer coupling, and the long time required to acquire relaxation rate dispersions, we conclude that MLV suspensions are not suitable for study by ^{1}H NMR relaxometry.

The success of our approach in reproducing the experimental relaxation dispersions demonstrates that our method is sensitive in particular to the differences in κ and D, between DMPC and DOPC which dominate the low frequency part of the relaxation dispersions. The literature suggests that dissolving other lipids, or lipophilic solutes, in lipid bilayers significantly alters both of these properties.[5,52] Hence the application of our approach to LUV systems of more complex composition may provide new insights into the influence of lipid type on membrane properties and function. Given current computational limitations, simulations[44] are limited to 100 ns, which is equivalent to ~10 MHz. Therefore, at the present time computational approaches cannot provide reliable information about such slow processes.

Conclusions

In summary, we have developed a systematic evidence-based approach to interpreting the motions in simple membrane systems. We find that ^{1}H relaxation data for LUVs can be interpreted in terms of order fluctuations (induced by shape fluctuations of the liposphere), translational diffusion on curved surfaces, rotational diffusion, and fast molecular dynamics, which are all physically reasonable and determined using known experimental values, where possible. We also find that inclusion of cross-correlations between the different dynamic modes is not required to reproduce the experimental data, which strongly supports our assumption that these are minor contributors to the total spectral density.

Our incremental approach is appropriate as it minimizes the number of components included in the interpretation, so it may in time be developed to interpret dynamics in more complex multicomponent membranes. In forthcoming work, we will present analysis of the size and temperature dependence of the relaxation dispersion for DMPC LUVs. This will further establish our approach and allow critical assessment of its potential for the study of viscoelastic properties of more complex LUV formulations.

Acknowledgment. This work was partially supported by funds from Foncyt (PICT25765), CONICET (PIP6420), and Secyt-UNC from Argentina. C.J.M. acknowledges the National Institute for Cellular Biotechnology and Enterprise Ireland (PC/2006/207) for financial support. D.B. also acknowledges Enterprise Ireland (IF/2001/364, PC/2004/0429) and the Higher Education Authority of the Republic of Ireland for supporting the purchase of NMR equipment. J.P. and E.F. acknowledge a fellowship granted by CONICET. The authors also acknowledge Dr. Guillermo Montich and CIQUIBIC - CONICET for support and access to infrastructure for preparing the liposome samples in Córdoba. C.J.M. and J.P. contributed equally to this work.

References and Notes

(1) Gawrisch, K. *The Structure of Biological Membranes. The Dynamics of Membrane Lipids*; Yeagle, P. L., Ed.; CRC Press: New York, 2005; p 540.
(2) Lee, G. M.; Jacobson, K. *Cell Lipids. Lateral Mobility of Lipids in Membranes*; Hoekstra, D., Ed.; Academic Press: New York, 1994; p 638.
(3) Simons, K.; Ikonen, E. *Nature* **1997**, *387*, 569.
(4) Crane, J. M.; Tamm, L. K. *Biophys. J.* **2004**, *86*, 2965.
(5) Filippov, A.; Orädd, G.; Lindblom, G. *Biophys. J.* **2003**, *84*, 3079.
(6) Filippov, A.; Orädd, G.; Lindblom, G. *Langmuir* **2003**, *19*, 6397.
(7) *Membrane Spectroscopy*; Grell, E., Ed.; Springer Verlag: Berlin, 1981.
(8) Kornberg, R. D.; McConnell, H. M. *Biochemistry* **1971**, *10*, 1111.
(9) Chan, S. I.; Feigenson, G. W; Seiter, C. H. A. *Nature* **1971**, *231*, 110.
(10) Charvolin, J.; Rigny, P. *J. Magn. Reson.* **1971**, *4*, 40.
(11) Wennerstrom, H. *Chem. Phys. Lett.* **1973**, *18*, 41.
(12) Bloom, M.; Burnell, E.; Valic, M. I.; Weeks, G. *Chem. Phys. Lipids* **1975**, *14*, 107.
(13) Kimmich, R.; Peters, A. *J. Magn. Reson.* **1975**, *19*, 144.
(14) Kimmich, R.; Voigt, G. *Chem. Phys. Lett.* **1979**, *62*, 181.
(15) Kimmich, R.; Schnur, G.; Scheuermann, A. *Chem. Phys. Lipids* **1983**, *32*, 271.
(16) Marqusee, J. A.; Warner, M.; Dill, K. *J. Chem. Phys.* **1984**, *81*, 6404.
(17) Rommel, E.; Noack, F.; Meier, P.; Kothe, G. *J. Phys. Chem.* **1988**, *92*, 2981.
(18) Halle, B.; Jóhannesson, H.; Venu, K. *J. Magn. Reson.* **1998**, *135*, 1.
(19) Vilfan, M.; Althoff, G.; Vilfan, I.; Kothe, G. *Phys. Rev. E* **2001**, *64*, 022902.
(20) Halle, B. *J. Chem. Phys.* **1991**, *94*, 3150.
(21) Lipari, G.; Szabo, A. *J. Am. Chem. Soc.* **1982**, *104*, 4546.
(22) King, R.; Jardetzky, O. *Chem. Phys. Lett.* **1978**, *55*, 15.
(23) Kimmich, R.; Anoardo, E. *Prog. NMR Spectrosc.* **2004**, *44*, 257.
(24) Perlo, J.; Anoardo, E. *J. Magn. Reson.* **2006**, *181*, 262.
(25) Perlo, J.; Barberis, L.; Anoardo, E., unpublished.
(26) Koynova, R.; Caffrey, M. *Biochim. Biophys. Acta* **1998**, *1376*, 91.
(27) Abragam, A. *Principles of Nuclear Magnetism*; Oxford: U. P. London, 1961.
(28) Freed, J. H. *J. Chem. Phys.* **1977**, *66*, 4183.
(29) Kruijff, B.; Wirtz, K. W. A. *Biochim. Biophys. Acta* **1977**, *255*, 311.
(30) Henriksen, J.; Rowat, A. C.; Ipsen, J. H. *Eur. Biophys. J.* **2004**, *33*, 732.
(31) Althoff, G.; Frezzato, D.; Vilfan, M.; Stauch, O.; Schubert, O.; Vilfan, I.; Moro, G. J.; Kothe, G. *J. Phys. Chem. B* **2002**, *106*, 5506.
(32) Althoff, G.; Stauch, O.; Vilfan, M.; Frezzato, D.; Moro, G. J.; Hausser, P.; Schubert, R.; Kothe, G. *J. Phys. Chem. B* **2002**, *106*, 5517.
(33) Lindblom, G.; Wennerström, H.; Arvidson, G. *Int. J. Quantum Chem.* **1977**, *S2*, 153.
(34) Bloom, M.; Evans, E.; Mouritsen, O. G. *Q. Rev. Biophys.* **1991**, *24*, 293.
(35) Lindblom, G.; Orädd, G. *Prog. Nucl. Magn. Reson. Spectrosc.* **1994**, *26*, 483.
(36) Saffman, P. G.; Delbruch, M. *Proc. Nat. Acad. Sci.* **1975**, *72*, 3111.
(37) Almeida, P. F.; Vaz, W. L.; Thompson, T. E. *Biophys. J.* **2005**, *88*, 4434.
(38) *Handbook of Chemistry and Physics*, 74th ed.; Lide, D., Ed.; 1993−1994.

(39) Umegawa, Y.; Matsumori, N.; Oishiv, T; Murata, M. *Biochemistry* **2008**, *47*, 13463.
(40) Duwe, H. P.; Sackmann, E. *Physica A* **1990**, *163*, 410.
(41) Mishra, V. K.; Anantharamaiah, G. M.; Segrest, J. P.; Palgunachari, M. N.; Chaddha, M. *J. Biol. Chem.* **2006**, *281*, 6511.
(42) Tamm, K.; McConnell, H. M. *Biophys. J.* **1985**, *47*, 105.
(43) Petersen, N. O.; Chan, S. I. *Biochemistry* **1977**, *16*, 2657.
(44) Lindahl, E.; Edholm, O. *J. Chem. Phys.* **2001**, *115*, 4938.
(45) Tristram-Nagle, S.; Petrache, H. I.; Nagle, J. F *Biophys. J.* **1998**, *75*, 917.
(46) Liu, Y.; Nagle, J. F. *Phys. Rev. E* **2004**, *69*, 040901.
(47) Przybylo, M.; Sýkora, J.; Humpoličková, J.; Benda, A.; Zan, A.; Hof, M. *Langmuir* **2006**, *22*, 9096.
(48) Kahya, N.; Scherfeld, D.; Bacia, K.; Schwille, P. J. *Struct. Biol.* **2004**, *147*, 77.
(49) Scherfeld, D.; Kahya, N.; Scwille, P. *Biophys. J.* **2003**, *85*, 3758.
(50) Nagle, J. F.; Tristram-Nagle, S. *Biochim. Biophys. Acta* **2000**, *1469*, 159.
(51) Alves, M.; Peric, M. *Biophys. Chem.* **2006**, *122*, 66.
(52) Chen, Z.; Rand, R. P *Biophys. J.* **1997**, *73*, 267.

JP907084S